

Fiber Orientation in the Canine Left Ventricle during Diastole and Systole

By Daniel D. Streeter, Jr., S.M., Henry M. Spotnitz, M.D.,

Dali P. Patel, M.D., Ph.D., John Ross, Jr., M.D., and Edmund H. Sonnenblick, M.D.

ABSTRACT

Fiber orientation across the left ventricular myocardial wall has been studied. Specimens were obtained from 18 dog hearts rapidly fixed in situ in systole, in diastole, and in dilated diastole. Fiber orientation was determined across the free wall at eight sites from a T-shaped specimen by measurements with light microscopy in serial paraffin sections. Results indicate: (1) The wall has a well-ordered distribution of fiber angles varying from about 60° (from the circumferential direction) at the inner surface to about -60° on the outer surface. The greatest change in angle with respect to wall thickness occurs at the two surfaces (endocardial and epicardial). (2) Fiber angles did not change significantly during the transition from diastole to systole, despite a 28% increase in wall thickness (except in the papillary muscle root region). (3) The proportion of fibers lying in the sector of fiber angles oriented circumferentially ($0 \pm 22.5^\circ$) to those oriented longitudinally (67.5 to 90° and -67.5 to -90°) is approximately 10:1. This ratio increases toward the base and diminishes toward the apex of the left ventricle. (4) All fiber angles in the lateral wall of hearts in systole increased through the wall by approximately 7° near the base and 19° near the apex relative to their counterparts in diastole, indicating bending or torsion of the left ventricle during contraction.

ADDITIONAL KEY WORDS distribution of fiber angles shear strain
fiber-wound pressure vessel myocardial continuum
left ventricular lateral wall structure

■ The distribution of stresses in the left ventricular wall is a function not only of the fiber tension but also of the spatial orientation of the fibers. Recent studies of serial sections have shown that the myocardial wall may be regarded as a well-ordered, fiber-wound continuum (1, 2) of intercon-

necting muscle fibers. The wall is characterized by gradual changes of fiber angle from endocardium to epicardium. There are no distinct bands of muscle and no discernible dividing septa such as have been claimed by anatomists since the time of Vesalius [1514] from studies using unwinding techniques now referred to as the Mall-MacCallum method (3, 4, 5). Indeed, the concept that an assembly of fiber bundles can be separated and its parts unravelled has been challenged in the past (6, 7) because the fiber matrix can be partitioned into different bundles depending on the orientation of the tearing forces employed. The serial section studies made recently in the dog heart (8) and in the pig heart (1) more accurately define fiber orientation but have not demonstrated the effects of ventricular contraction

From the Section on Clinical Biophysics and the Cardiology Branch, National Heart Institute, Bethesda, Maryland 20014.

This work was supported in part by U. S. Public Health Service Research Grant HE 5454-08 from the National Heart Institute.

Dr. Ross's present address is Department of Medicine, University of California, San Diego, La Jolla, California 92037.

Dr. Sonnenblick's present address is Cardiovascular Unit, Peter Bent Brigham Hospital, Boston, Massachusetts 02115.

Received October 16, 1968. Accepted for publication December 20, 1968.

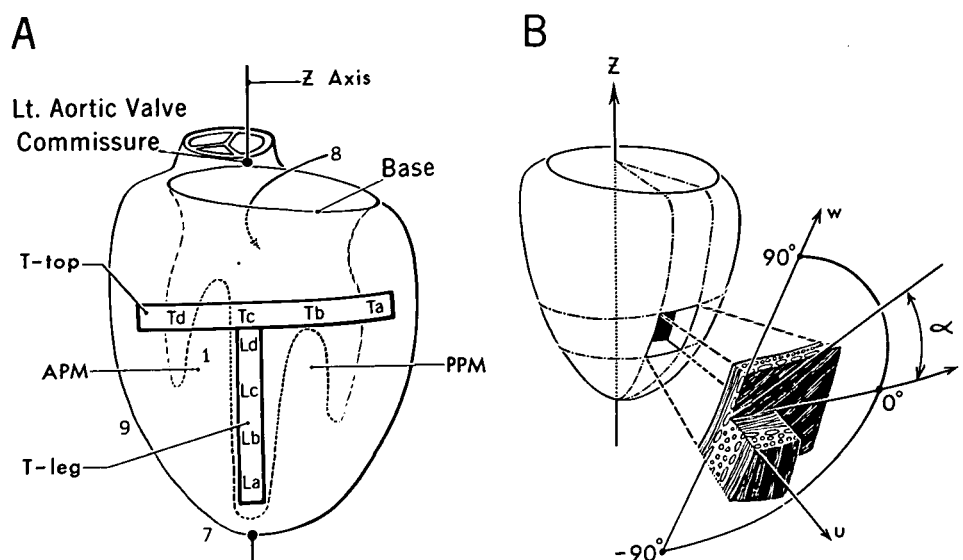


FIGURE 1

A: Left ventricular free wall with T-shaped full-thickness specimen before removal. APM is the anterior papillary muscle and PPM is the posterior papillary muscle. The top of the T extends from the basilar region near but excluding the anterior papillary muscle root to the posterior demarcation of the right and left ventricular walls. The leg of the T extends longitudinally between the two papillary muscles from the top of the T toward the ventricular apex. Lettering identifies eight sites for measurement of fiber orientation. Numbers indicate additional sampling sites: 1 includes the root of APM, 7 is on the same meridian as 9, almost at the apex and anterior to the root of APM, 8 is on the interventricular septum just basilar to the most anterior right ventricular papillary muscle, and 9 is on the left ventricular side of the anterior descending coronary artery midway between apex and base. B: Schematic drawing showing a full-thickness specimen removed from wall of left ventricle. Local axes u , v and w on the specimen are defined by the local normal, latitude and longitude, respectively, for a given site on the epicardial surface. Fiber angle, α , is positive when measured counterclockwise from the local v -axis. Note that the local w -axis is not necessarily parallel to the z -axis.

and do not permit conclusions regarding possible alterations of fiber position during the cardiac cycle. Accordingly the present study was directed to the systolic and diastolic geometry of the fiber continuum in the left ventricle of the dog heart.

Methods

Previous studies in this laboratory provided three groups of hearts of matched left ventricular (LV) weight that had been fixed with glutaraldehyde at known phases of the cardiac cycle (9, 10). These hearts represented physiologic systole (7 hearts, mean LV cavity volume 20.2 ml, mean LV weight 102.4 g), diastole (6 hearts, mean LV cavity volume 51.6 ml, mean LV weight 95.5 g), and dilated diastole (5 hearts, mean LV cavity volume 72.1 ml, mean LV weight 108.3 g). Each heart was sup-

ported in a wooden frame along its major reference axis, chosen to pass from the left ventricular apex to the mitral aspect of the left aortic valve commissure (1, 11, 12). With the heart transfixed on this frame by long pins passing through the walls of the left ventricle into a silicone rubber cast of the ventricular chamber (9), a tool rest facilitated cutting anywhere into the surface of the ventricle along lines of longitude or lines of latitude relative to the major axis. T-shaped, full-thickness specimens, 3 mm wide, were thereby obtained from 14 hearts (5 in systole, 5 in diastole, 4 in dilated diastole) extending over nearly the full width of the left ventricular wall from right to left and from apex to base (Fig. 1, A). In five hearts small windows were made by cutting blocks 8 × 8 mm through the left ventricular wall in a number of regions (sites Lb, Tc, 1, 7, 8, and 9 in Fig. 1, A).

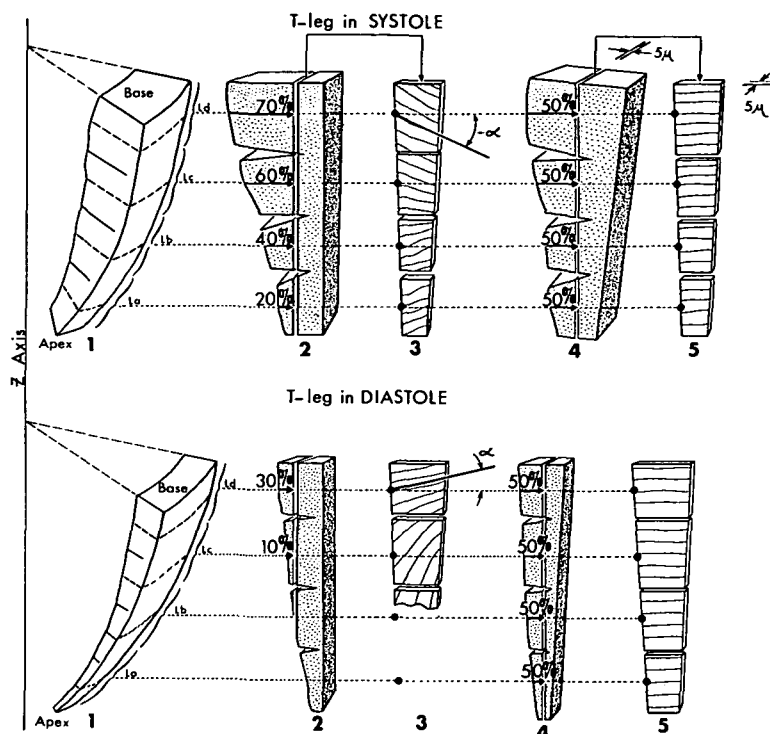


FIGURE 2

Comparable systolic and diastolic T-leg specimens as they appear in the LV free wall (1); side view after flattening (2) shows a representative section, 5μ thick, 3 mm in from, and parallel to, the epicardium. Percents shown represent the distance from the endocardium of this section as a percent of wall thickness. Since this plane represents a variable fraction of total wall thickness, fiber angle, α , is not constant from apex to base in the section (3). A plane at a given constant fraction of wall thickness (4) reveals a relatively constant fiber orientation at all sampling sites. 5 shows fiber orientation at midwall (50% of the wall thickness).

Radial slits permitted the curvature of the T-shaped specimens to be flattened (Fig. 2) before they were dehydrated in tetrahydrofuran and embedded in paraffin. Sequential sections parallel to the epicardium were cut by a microtome at a thickness of 5μ and stained with Gomori trichrome (13) for light microscopy. The angle formed between the myocardial fibers and the cut edge of the specimen could then be determined by using a microscope with a rotating stage and a revolving reticular eyepiece. Fiber angle, α , was measured in the plane parallel to the epicardium relative to a line of latitude. Fiber angles, viewed from the epicardial side, are positive in the upper right quadrant and negative in the lower right (Figs. 1, B, and 2). Zero degrees in this reference system is circumferential while $\pm 90^\circ$ is longitudinal, oriented from apex to base. Usually the angles were read from sections spaced 0.2 to 0.4 mm apart. Four measuring sites were

used across the top of the T, and four more on the leg, from apex to base (Fig. 1, A). Data analysis was facilitated by normalizing wall thickness so that radial position in the wall is expressed as percent of wall thickness from the endocardium (Fig. 2). This normalization procedure permits direct comparison of data independent of thickness variations in the same heart or different hearts.

Technical problems prevented measurements of fiber angle in less than 5% of the slides obtained. These difficulties included fragmentation of the reference edge by the cutter as well as the presence of obliquely sectioned fibers having a component of length that was normal to the plane sectioned by the microtome. The in-plane length component was at least four times the normal component in over 90% of systolic tissue sections and 95% of diastolic sections. Measurements were generally reproducible from observer to observer (to within $\pm 10^\circ$)

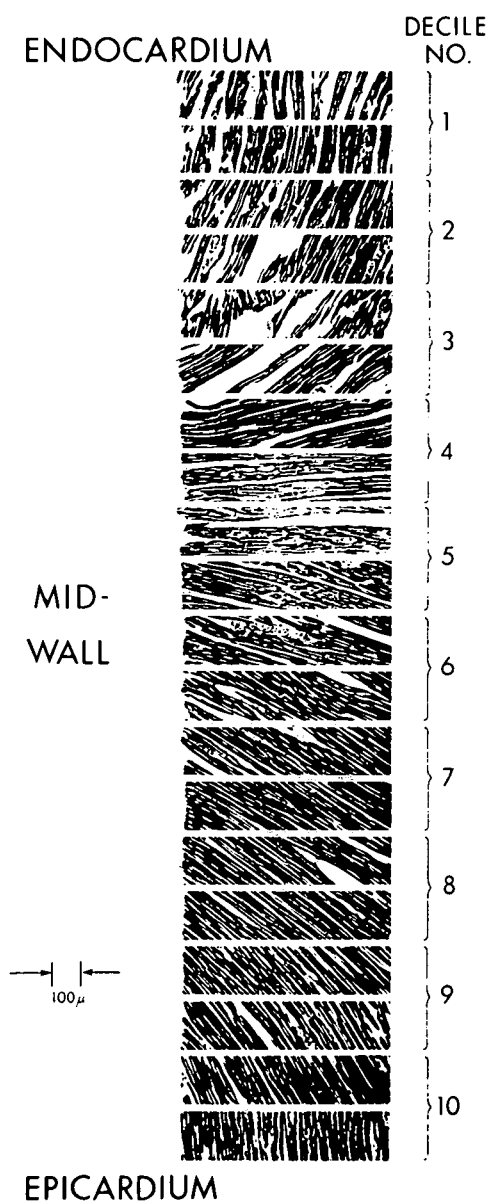


FIGURE 3

Typical sequence of photomicrographs showing fiber angles in successive sections taken from a heart in systole at region Tc. The sections are parallel to the epicardial plane. Fiber angle is $+90^\circ$ at the endocardium, running through 0° at the midwall to -90° at the epicardium. The sequence of numbers refers to deciles of wall thickness.

within 5 mm of a given sampling point. Shrinkage of the preparation due to dehydrating, embedding, and sectioning by microtome was ap-

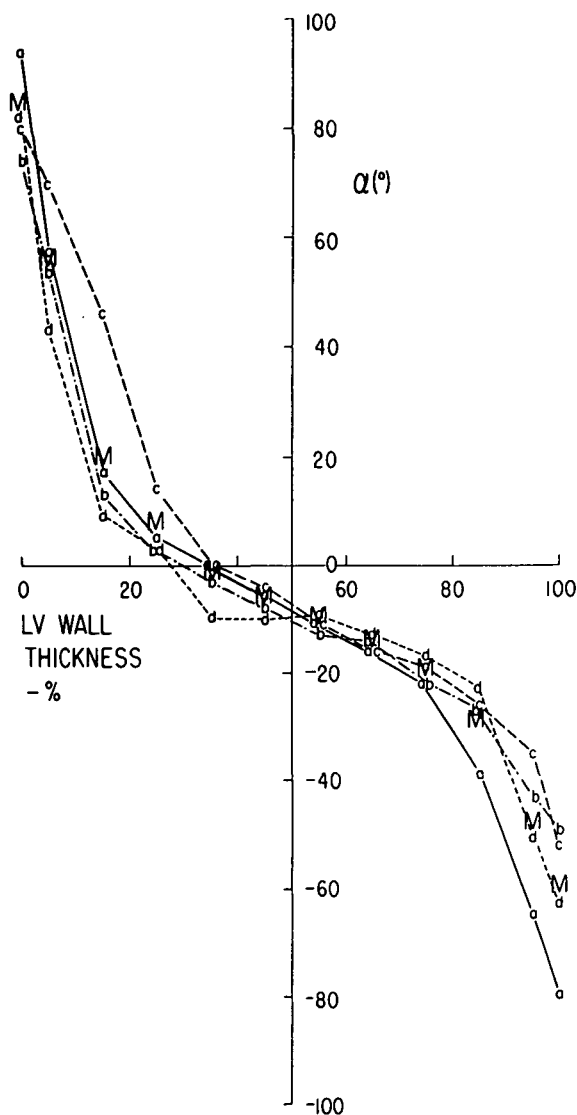


FIGURE 4

Fiber angles for four sampling sites, a through d, in a T-top section from a heart in diastole are plotted as a function of percent wall thickness. Zero percent of wall thickness implies the endocardial surface. M represents the mean of the data at these four sites.

proximately 18% in the fiber plane parallel to the epicardium.

Results

An example of the change of fiber angle through the wall at a single sampling point in the left ventricle is shown in Figure 3 by

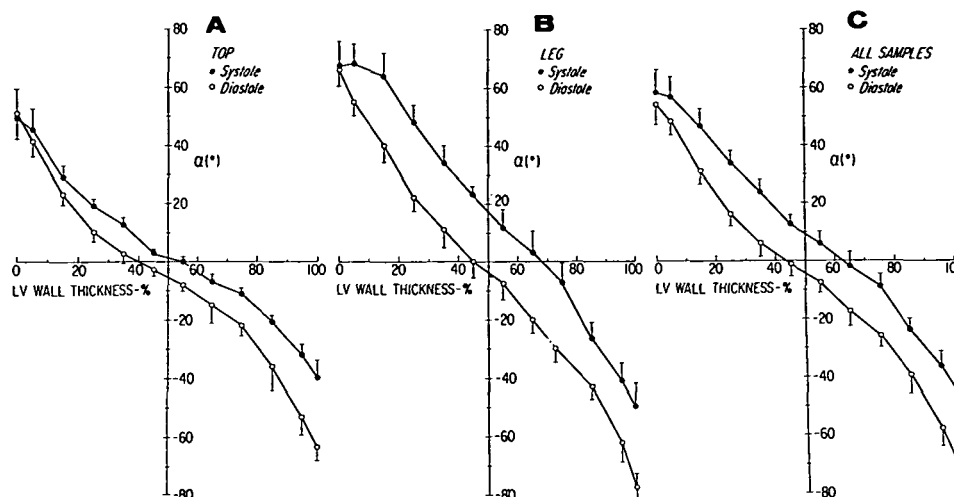


FIGURE 5

Averaged data from five hearts in systole compared with averaged data from five hearts in diastole showing fiber angle distribution through the wall (normalized). Zero percent of wall thickness implies the endocardial surface. The standard error of the mean is shown in each decile of wall thickness. Note that all fiber angles in the systolic hearts increased through the wall by an approximately constant angle relative to their counterparts in diastole.

a representative sequence of photomicrographs of the sections cut by the microtome. A continuous distribution with no discrete fiber bundles is evident. In Figure 4 are typical plots of fiber angle vs. percent wall thickness. The extremes of fiber angle tend to approach 90° at the endocardium and -90° at the epicardium.

The effect of the transition from diastole to systole on the fiber angle-wall thickness relations is illustrated in Figure 5, where five systolic hearts are compared with five diastolic hearts. The fiber angle, α , changes smoothly across the wall in both systole and diastole. Generally, the change in angle with respect to the normalized wall thickness ($d\alpha/dh$) is greatest near the endocardial and epicardial surfaces. Most fibers are oriented within $\pm 45^\circ$ of the circumference.

The transition from diastole to systole is associated with a constant increase in all fiber angles through the wall at any one sampling site. This increase averages 7° in the T-top (Fig. 5, A), and 19° in the T-leg

(Fig. 5, B). This may be attributed to either bending of the Z-axis during contraction (9) or torsional rotation of the entire free wall relative to the base or septum.

To determine possible relative angular displacements within the fiber continuum itself, a constant angle as determined at midwall was subtracted from each fiber angle curve to shift them all to 0° at midwall. In general, significant differences could not be demonstrated ($P > .05$) between the systolic, diastolic, or dilated diastolic hearts. However, in two of the eight sampling sites, La and Lb, significant fiber angle differences were observed ($P < .05$) between systole, diastole, and dilated diastole; $d\alpha/dh$ changed, i.e., shearing strain¹ appeared in the endocardial third of the wall. These changes for site La are shown in Figure 6.

In Figure 7 the systolic and diastolic data

¹Shearing strains between adjacent myocardial fibers through the wall can occur either by rotational or translational displacement (14, 15) between the fibers. We can only measure shearing strains due to rotational displacement in this study.

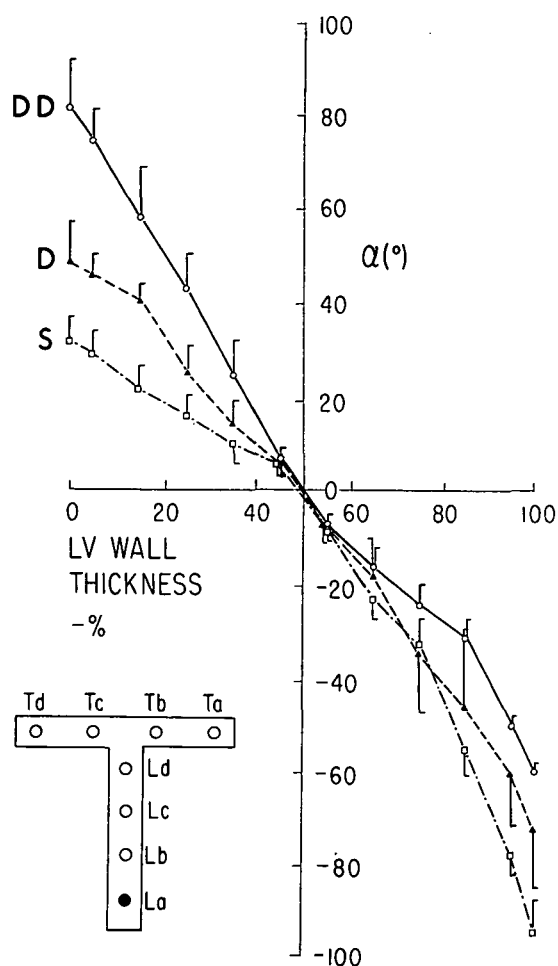


FIGURE 6

Plots of fiber angle, α , vs wall thickness at site La (Fig. 1). Data are averaged from five hearts in systole (S) and four each in diastole (D) and dilated diastole (DD). Zero percent wall thickness implies the endocardial surface. Standard errors of the mean are shown. Curves have been shifted to zero degrees at midwall to eliminate rigid body motion. Note differences in shape and slope of curves. This is atypical of the general observations (Fig. 5) and suggests shearing strain in the apical wall region of the papillary muscle roots, especially near the endocardium.

are averaged together. The fiber angle vs. percent wall thickness from 10 hearts, 5 in systole and 5 in diastole, is plotted for various combinations of the same eight sampling locations in the T specimen. In A (Fig. 7) the top of the T (4 sites) is compared with the leg (4 sites). Significant differences

($P < .05$) can be observed in the fiber angle, α , in the endocardial half of the wall thickness. The average slope is steeper in the leg of the T than it is in the top of the T, indicating relatively more longitudinally oriented fibers in the T-leg than in the T-top. B and C (Fig. 7) show similarly shaped curves for the right and left halves of the T-top, and apical and basilar halves of the T-leg, respectively, indicating no essential difference in slopes.

The distribution of fibers according to four possible modes of orientation in the T-top, T-leg, and entire T is represented by bar graphs in Figure 8. The height of the bars illustrates the percent of fibers oriented in the left-hand oblique mode (Group I, $-45 \pm 22.5^\circ$), the circumferential mode (Group II, $0 \pm 22.5^\circ$), the right-hand oblique mode (Group III, $45 \pm 22.5^\circ$), and the longitudinal mode (Group IV, 67.5 to 90° and -67.5 to -90°). Note that fibers having a longitudinal mode of orientation exist in both the endocardial and epicardial regions of the wall. Data from systolic, diastolic, and dilated diastolic hearts are included in this figure. The bar graphs show that the smallest proportion of fibers falls into the longitudinal mode while the greatest proportion is oriented in the circumferential mode with roughly equal portions distributed into each of the two oblique modes. As defined, the ratio of fibers in the circumferential mode to fibers in the longitudinal mode is approximately 10:1, increasing toward the base and decreasing toward the apex.

In five hearts, systolic and diastolic data were also obtained from small window samples cut through the wall of the left ventricle 5 to 15 mm from the apex (location 7 in Fig. 1). The general relationships of the fibers within the wall are similar to those obtained in the T-leg. Although there was a predominance of the circumferentially oriented fibers near the apex, this predominance was not as great as that observed in myocardium closer to the base.

The general range and distribution of fiber angles observed in the T-specimens were

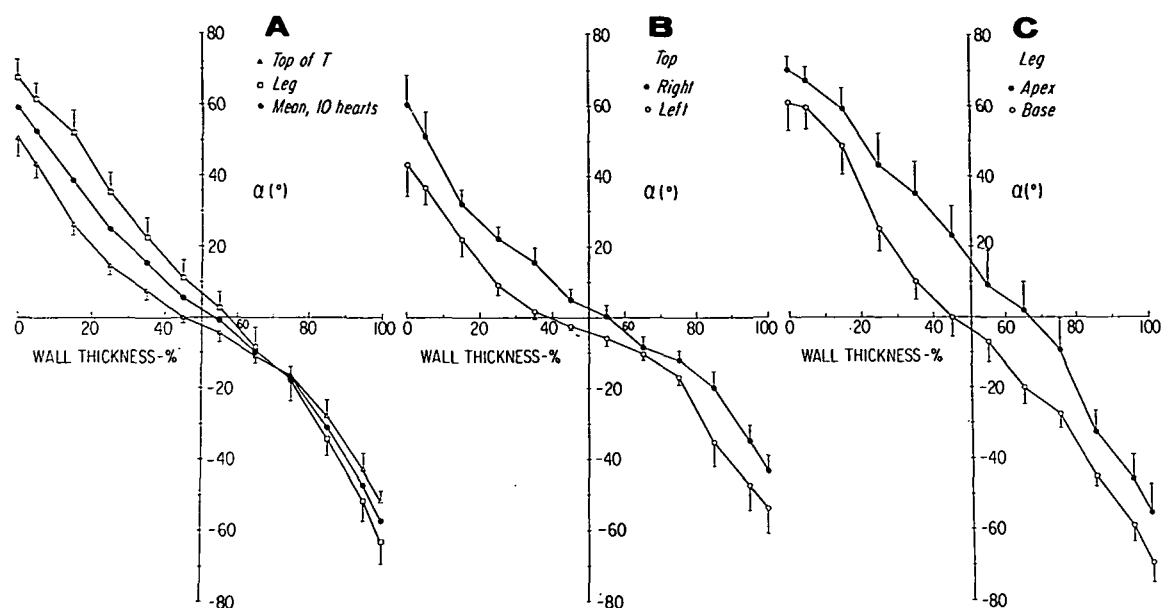


FIGURE 7

Data on fiber angles from five systolic and five diastolic hearts averaged together and plotted as a function of percent wall thickness to demonstrate regional variations in the left ventricular wall. Zero percent wall thickness implies the endocardial surface. Standard errors of the mean are shown. A shows significant differences in fiber orientation between the T-top and T-leg in the endocardial half of the wall. B and C show similar shapes for the right and left halves of the T-top, and apical and basilar halves of the T-leg, respectively. Note the relatively constant change in angle through the wall in each of these panels.

similar to those observed in other selected areas of the left ventricle, including the ventricular septum. Local peculiarities consistent with earlier results (1) were observed, including plateaus of 90° fiber angles in the roots of papillary muscles. At all other sampling regions (1, 7, 8, 9 in Fig. 1) a well-defined, smoothly changing fiber orientation was demonstrated.

Discussion

Despite much detailed investigation of the fiber structure of the left ventricular wall (3-7), the smooth transition of fiber angle from endocardium to epicardium has only recently been emphasized (1, 8). The spatial relations of the fibers in serial microscopic sections suggest that the left ventricle for purposes of stress analysis (2) can be characterized as a cross-linked, fiber-wound ellipsoidal or paraboloidal pressure vessel

(16), with fiber angle changing smoothly from about 60° inside to about -60° outside. Significant changes in fiber angle between diastole and systole were not generally observed.

While speculation regarding possible alterations in fiber orientation during ventricular contraction could not be resolved until the present, previous fiber angle studies suggested that major rearrangements did not occur between diastole and systole as simulated by rigor (8). In view of a 28% greater wall thickness in systolic than in diastolic hearts (9), the relative stability of the sequence of fiber angles in the wall of the left ventricle is remarkable. Such an increase in wall thickness necessitates a rolling movement of one fiber upon another (8, 17) and is associated with the appearance of small but measurable shear strains which are most significant in the second and third deciles of wall thick-

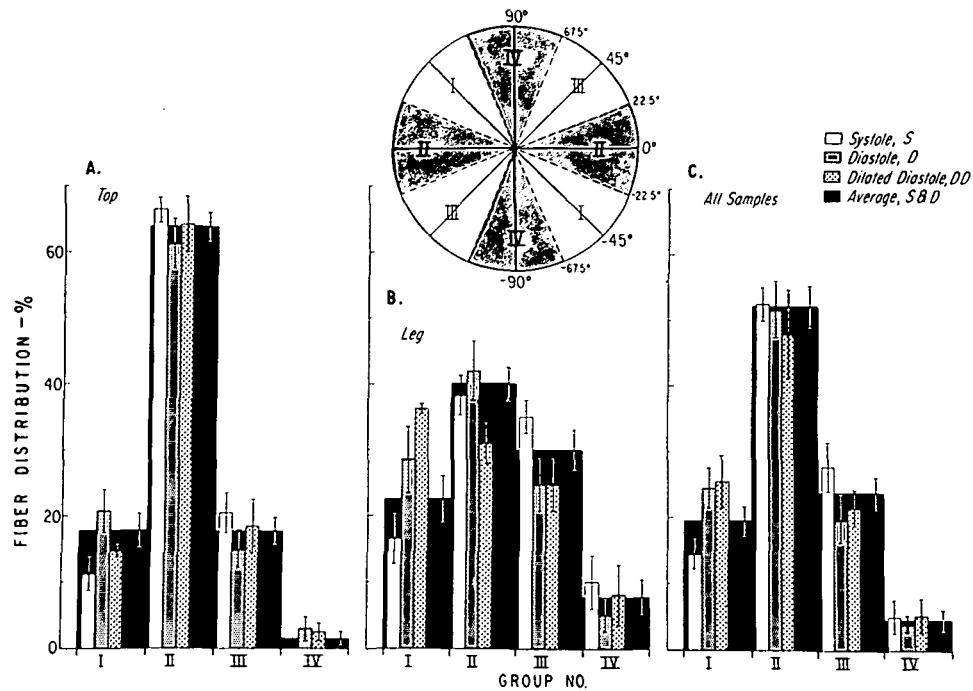


FIGURE 8

The distribution of fibers by groups representing each of four possible modes of fiber orientation. As shown in the inset, Group I represents the left-hand oblique mode of orientation ($-45 \pm 22.5^\circ$), Group II the circumferential mode ($0 \pm 22.5^\circ$), Group III the right-hand oblique mode ($45 \pm 22.5^\circ$) and Group IV the longitudinal mode (67.5 to 90° and -67.9 to -90°). Thus each mode encompasses 45° of arc. Note that fibers having a longitudinal mode of orientation exist in both the endocardial and epicardial regions of the wall. The height of the bars indicates the proportion of fibers in each group. The broad solid bars represent data averaged for systole and diastole. Averages for data of the subgroups are indicated by the narrow shaded bars. Standard errors of the mean are shown.

ness. In this study we observed shearing strains due to rotational displacement of adjacent fibers between systole and diastole only at sites La and Lb (Fig. 1A). Since our data measures only end points (systole or diastole), we cannot rule out transiently occurring shearing strains during the cardiac cycle. Moreover, shearing strains due to translational displacement of adjacent fibers could occur without any change in fiber angle.

It is not possible in all cases to find and measure the fiber orientation in the region just inside the epicardium and endocardium. Visual examination of the surfaces of an entire left ventricle indicates that $\pm 90^\circ$ (1)

is more closely approached than our measurements indicate. Because these fibers were missed in the first and last few sections cut by microtome (where the rate of change of fiber angle is very great), the average surface angle values measured are somewhat smaller than might be expected.

Acknowledgments

We are grateful to Dr. Donald L. Fry and Dr. Eugene Braunwald for their help and criticism, and to Mr. Charles E. Baker, Miss Pat Kenny, Mr. Fred Plowman, and Mr. Walter G. P. Seewald for their technical assistance. For initial preparation of the glutaraldehyde-fixed hearts we are indebted to Dr. James W. Covell and Dr. Gerard Kaiser, with the technical assistance of Robert Lewis, Richard McGill, and Noel Roane.

References

1. STREETER, D. D., JR., AND BASSETT, D. L.: An engineering analysis of myocardial fiber orientation in pig's left ventricle in systole. *Anat. Rec.* 155: 503, 1966.
2. RUSHMER, R. F., VAN CITTERS, R. L., AND FRANKLIN, D. L.: Some axioms, popular notions, and misconceptions regarding cardiovascular control. *Circulation* 27: 118, 1963.
3. MACCALLUM, J. B.: On the muscular architecture and growth of the ventricles of the heart. *Welch Festschrift, Johns Hopkins Hosp. Rept.* 9: 307, 1900.
4. MALL, F. P.: On the muscular architecture of the ventricles of the human heart. *Am. J. Anat.* 11: 211, 1911.
5. ROBB, J. S., AND ROBB, R. D.: The normal heart: Anatomy and physiology of the structural units. *Am. Heart J.* 23: 455, 1942.
6. LEV, M., AND SIMKINS, C. S.: Architecture of the human ventricular myocardium: Technique for study using a modification of the Mall-MacCallum method. *Lab. Invest.* 5: 395, 1956.
7. GRANT, R. P.: Notes on the muscular architecture of the left ventricle. *Circulation* 32: 301, 1965.
8. HORT, W.: Makroskopische und mikrometrische Untersuchungen am Myokard verschieden stark gefüllter linker Kammern. *Arch. Pathol. Anat. Physiol.* 333: 523, 1960.
9. ROSS, J., JR., SONNENBLICK, E. H., COVELL, J. W., KAISER, G. A., AND SPIRO D.: Architecture of the heart in systole and diastole: Technique of rapid fixation and analysis of left ventricular geometry. *Circulation Res.* 21: 409, 1967.
10. SONNENBLICK, E. H., ROSS, J., JR., COVELL, J. W., SPOTNITZ, H. M., AND SPIRO D.: Ultrastructure of the heart in systole and diastole: Changes in sarcomere length. *Circulation Res.* 21: 423, 1967.
11. GRANT, R. P.: Architectonics of the heart. *Am. Heart J.* 46: 405, 1953.
12. KERR, A., JR., AND GOSS, C. M.: Retention of embryonic relationship of aortic and pulmonary valve cusps and a suggested nomenclature. *Anat. Record* 125: 777, 1956.
13. GOMORI, G.: A rapid one-step trichrome stain. *Am. J. Clin. Pathol.* 20: 661, 1950.
14. RUSHMER, R. F., CRYSTAL, D. K., AND WAGNER, C.: Functional anatomy of ventricular contraction. *Circulation Res.* 1: 162, 1953.
15. FEIGL, E. O., AND FRY, D. L.: Intramural myocardial shear during the cardiac cycle. *Circulation Res.* 14: 536, 1964.
16. FRY, D. L., GRIGGS, D. M., JR., AND GREENFIELD, J. C., JR.: Myocardial mechanics: Tension-velocity-length relationships of heart muscle. *Circulation Res.* 14: 73, 1964.
17. LINZBACH, A. J.: Heart failure from the point of view of quantitative anatomy. *Am. J. Cardiol.* 5: 370, 1960.